

PAPER

Temperature dependence of voltage-controlled polarization plane rotation in a magnetic and electro-optic heterostructure



To cite this article: Yuliya S Dadoenkova *et al* 2019 *Phys. Scr.* **94** 105006

View the [article online](#) for updates and enhancements.

Recent citations

- [Magnetic field detection using a highly sensitive FBG probe](#)
Alireza Samavati *et al*

Temperature dependence of voltage-controlled polarization plane rotation in a magnetic and electro-optic heterostructure

Yuliya S Dadoenkova^{1,2} , Florian F L Bentivegna²  and Sergey G Moiseev^{1,3} 

¹Ulyanovsk State University, 432017, Ulyanovsk, Russia

²Lab-STICC (UMR 6285), CNRS, ENIB, F-29238 Brest Cedex 3, France

³Kotelnikov Institute of Radio Engineering and Electronics of the Russian Academy of Sciences, Ulyanovsk Branch, 432011, Ulyanovsk, Russia

E-mail: y.dadoenkova@gmail.com

Received 27 December 2018, revised 21 May 2019

Accepted for publication 6 June 2019

Published 6 August 2019



Abstract

We propose a theoretical study of the influence of temperature on the state of polarization of a near-infrared light beam reflected from or transmitted through a voltage-controlled nematic liquid crystal (LC) cell deposited on a magnetic film. In both cases, the change in polarization with respect to that of the incoming beam originates in the linear Kerr or Faraday effects taking place in the magnetic layer, but the overall value of the polarization plane rotation depends on the reflectivity and transmittivity of the whole heterostructure. Temperature manifests itself in all layers of the structure through both thermal expansion and the thermo-optic effect when it varies between room temperature and the temperature of nematic-isotropic phase transition in the LC. The thermo-optic effect is strongest in the LC cell, where it is shown to induce noticeable variations of the polarization plane rotation of both reflected and transmitted light beams in that temperature range. Such temperature-dependent changes of the magneto-optical response can be compensated for by adjusting the dc voltage applied to the LC. On the other hand, we show that they may be exploited for sensitive temperature monitoring.

Keywords: functional materials, Kerr rotation, Faraday rotation, polarization plane rotation, control of light polarization

(Some figures may appear in colour only in the online journal)

1. Introduction

The magneto-optical Kerr and Faraday effects were historically defined as the rotation of the polarization plane of a linearly-polarized optical beam respectively reflected from and transmitted through a magnetic material. More generally, they refer to the modification, upon reflection or transmission, of the state of polarization of a polarized electromagnetic wave when it interacts with any magnetic medium or structure including magnetic materials. These well-known effects are widely used for a variety of applications, including the investigation of the magnetic structure of thin magnetic films and magnetic multilayers [1–3], such devices as circulators or

phase shifters [1], magnetic sensors [4], or even for chemical detection [5, 6]. For most of these applications, it can be useful to be able to control and enhance the Kerr or Faraday angle using external excitations, which can be achieved by including functional materials in the devices, i.e. materials whose properties (in particular, their permittivity and permeability) can be adjusted under the influence of such excitations. Recent studies of structures enabling tunable Kerr and Faraday effects include the description of electro-optic materials [7–10], magneto-photonics crystals [9–11], or plasmonic structures [12]. On the other hand, temperature has been shown to exert a potentially strong influence on the Kerr and Faraday effects. This has been investigated, both

theoretically and numerically, in various materials and structures, and over wide ranges of temperatures [13–22].

In this paper, we aim to investigate the control of the temperature-dependent polarization plane rotation of a light beam upon reflection from or transmission through a simultaneously magnetic and electro-optic heterostructure, with a view to exploiting such a control for photonic devices (such as phase rotators or isolators) or for sensors. Specifically, the system under study is a heterostructure consisting of a nematic cyano-4'-pentylbiphenyl (5CB) liquid crystal (LC) cell deposited on an yttrium-iron garnet (YIG) magnetic film. Here, the magneto-optical Kerr and Faraday effects take place in the YIG film with uniform saturation magnetization $\pm \mathbf{M}_{\text{sat}}$. The fine tuning of the overall polarization rotation of an incident light beam is provided by the combination of that film with the LC cell. Indeed, the optical responses of such a heterostructure have been shown to be efficiently tuned with the dc voltage applied to the LC cell [23–25]. Thermal effects in the LC cell, however, must be accounted for, as they introduce a strong dependence of the magneto-optical response of the heterostructure on temperature variations. We study this dependence in the range between room temperature (20 °C) and the nematic-isotropic phase transition temperature (35.1 °C) of the LC under study [23, 26]. In that temperature range, the purely magneto-optical Kerr and Faraday rotations are not expected to vary much in the YIG layer magnetized at saturation. We show, however, that the temperature-induced drift of the polarization plane rotation, as a result of the intricate interaction of the light waves with the entire magneto-optical and electro-optical heterostructure, can be reduced or even annulled through a careful tuning of the applied dc voltage. Conversely, we suggest that the dependence of the polarization plane rotation upon thermal changes could be put to use for temperature monitoring.

The paper is organized as follows. In section 1, we present the geometry of the multilayered heterostructure and describe the influence of temperature on the structural and optical properties of its constituents, i.e. the LC cell, the indium tin oxide (ITO) electrodes that surround it, and the YIG film. In section 3, we discuss the results of our calculations. In particular, we compare the temperature-dependent polarization plane rotations obtained with the magnetic YIG film alone to those obtained when the electro-optic LC cell is adjoined to it. We subsequently discuss the possibility, and a potential application, of tuning, annulling, or enhancing these effects with the voltage applied to the LC cell, before summarizing our results in section 4.

2. System description and constitutive properties

2.1. Geometry of the system

The system consists of a bigyrotropic magnetic YIG film on which a LC cell of nematic 5CB, sandwiched between two thin ITO electrodes, is deposited (figure 1). The interfaces separating the materials are parallel to the (xy) plane of a Cartesian system of coordinates, and the lateral dimensions of

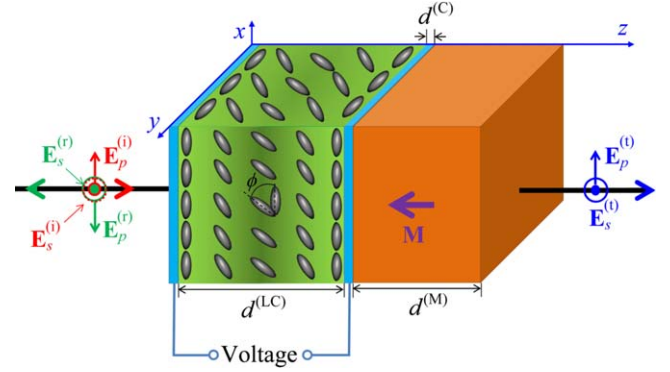


Figure 1. Schematic of the structure: LC cell between cladding electrodes on a magnetic film. $E_{\parallel,\perp}^{(i,r,t)}$ denote the components of the incident (i), reflected (r) and transmitted (t) optical electric fields directed parallel (\parallel) and perpendicular (\perp) to the (xz) plane along which LC molecules rotate, ϕ is the tilt angle of the LC molecules, and \mathbf{M} is the saturation magnetization in the magnetic film.

the layers are supposed to be much larger than their thickness, so that only the boundary conditions along the z -axis will be considered.

Magnetic saturation is reached in the YIG layer, in such a way that uniform and homogeneous magnetization \mathbf{M} either parallel or anti-parallel to the positive direction of the z -axis (in the following, we will refer to the parallel and anti-parallel polar configurations, respectively) is achieved. This magnetization can be reversed via the application of a static magnetic field. Hence, $\mathbf{M} = M\hat{z} = \pm M_{\text{sat}}\hat{z}$, where M_{sat} is the magnitude of the magnetization vector at saturation. The magnetization in YIG gives rise to the magneto-optical Kerr and Faraday rotations which manifest themselves through the polarization change of reflected and transmitted light, respectively [1, 2].

In the LC cell, a dc voltage V applied between the electrodes modifies the collective orientation of the elliptically shaped molecules parallel to the (xz) plane. This orientation is characterized by the tilt angle ϕ of their long axis with respect to the x -axis. Due to the anchoring of the molecules at the interfaces of the LC cell, variations of the tilt angle only take place when the dc voltage applied to the electrodes exceeds a threshold value V_{th} [27]. For $V > V_{\text{th}}$, the molecules rotate non-uniformly within the cell, and the variations of the tilt angle modify the components of the dielectric permittivity tensor of the LC. Thus, the optical response of the whole system can be controlled via the externally applied voltage.

A light beam of near-infrared wavelength λ_0 impinges the left-hand side of the structure under normal incidence, which corresponds to the polar magneto-optical configuration in terms of light interaction with the magnetic film [1]. The anisotropy of the LC alignment parallel to the (xz) plane leads us to consider the components of the optical fields parallel (\parallel) and perpendicular (\perp) to that plane. In the following, discussions of the polarization dependence of the optical response of the system will refer to the conventional s and p notations with respect to the (xz) plane thus considered as the plane of incidence.

In this paper, the dependence of the optical properties of the system upon temperature variations is taken into consideration. As a consequence, these variations must be accounted for in all the layers of the system. Specifically, the temperature dependence of the polarization plane rotation of the reflected and transmitted light beams is investigated. It manifests itself through (i) the thermal expansion of the layer thicknesses, which modifies the geometry of the system and, as a result, the optical path of the electromagnetic waves, and (ii) the thermo-optic effect, which affects the refractive indices of its constituents. The range of variation of the temperature T extends from room temperature $T_0 = 20^\circ\text{C}$ to the temperature $T_{\text{NI}} = 35.1^\circ\text{C}$ at which the LC exhibits a phase transition from the nematic to the isotropic phase. We assume that the local temperature is the same in all the layers and is equal to that of the air immediately surrounding the system. Its variations are also slow enough to ensure that all changes in thickness and permittivity experienced by the constituents of the structure are quasistatic.

We take the nominal thicknesses of the layers at temperature T_0 to be $d_0^{(\text{ITO})} = 0.07\ \mu\text{m}$, $d_0^{(\text{LC})} = 2.2\ \mu\text{m}$, and $d_0^{(\text{YIG})} = 3\ \mu\text{m}$, and we denote $L = d_0^{(\text{LC})} + 2d_0^{(\text{ITO})} + d_0^{(\text{YIG})}$ the nominal thickness of the system. The variation of the thickness with temperature T is characterized in each layer by the *thermal expansion* coefficient $\eta^{(k)}(T)$ (where $k = \text{ITO}, \text{LC}, \text{YIG}$) of the medium it is made of [23]. Within the range $[T_0, T_{\text{NI}}]$, the linear thermal expansion coefficients of YIG and ITO are virtually constant and equal to $\eta^{(\text{YIG})} = 1.04 \times 10^{-5}\ \text{K}^{-1}$ [28] and $\eta^{(\text{ITO})} = 10.2 \times 10^{-6}\ \text{K}^{-1}$ [29], respectively. They are one to two orders of magnitude smaller than that of 5CB, which varies nonlinearly with temperature, with $\eta^{(\text{LC})} \sim (3\text{--}6) \times 10^{-4}\ \text{K}^{-1}$ [30]. As a consequence, the influence on the optical path of the absolute variations of $d^{(\text{ITO})}$ and $d^{(\text{YIG})}$ within the $[T_0, T_{\text{NI}}]$ interval (approximately $4.5\ \text{\AA}$ and $10\ \text{\AA}$, respectively) is negligible. In comparison, the increase of $d^{(\text{LC})}$ is about $10\ \text{nm}$ and its influence cannot be neglected [23].

2.2. Material parameters of the constituents

Calculations are performed for $\lambda_0 = 1\ \mu\text{m}$. Both 5CB and YIG are transparent at this wavelength, whereas the ITO electrodes induce some losses. The latter are homogeneous and isotropic. The complex relative permittivity tensor elements of ITO are thus given by $\tilde{\varepsilon}_{jk}^{(\text{ITO})} = (\varepsilon^{(\text{ITO})} + i[\kappa^{(\text{ITO})}]^2)\delta_{jk}$, $(j, k) \in \{x, y, z\}^2$, where $\kappa^{(\text{ITO})}$ is the extinction coefficient of ITO and δ_{ij} is the Kronecker delta. The variation of real part $\varepsilon^{(\text{ITO})}$ with temperature (thermo-optic effect) is characterized by a constant thermo-optic coefficient $\gamma^{(\text{ITO})}$, with $\varepsilon^{(\text{ITO})}(\Delta T) = (n_0^{(\text{ITO})} + \gamma^{(\text{ITO})}\Delta T)^2$, where $n_0^{(\text{ITO})} = \sqrt{\varepsilon_0^{(\text{ITO})}}$ is the refractive index of the medium at nominal temperature T_0 . The numerical values used in section 3 are $\varepsilon_0^{(\text{ITO})} = 1.7057$, $\kappa^{(\text{ITO})} = 0.0337$ [28], and $\gamma^{(\text{ITO})} = 2.229 \times 10^{-4}\ \text{K}^{-1}$ [31].

The nematic LC cell consists of inhomogeneously aligned, uniaxial, rod-shaped molecules with real-valued principal relative permittivities $\varepsilon_1^{(\text{LC})}$ and $\varepsilon_2^{(\text{LC})} = \varepsilon_3^{(\text{LC})}$. The collective alignment of the molecules is assumed to be

parallel to the (xz) plane (figure 1) and to depend on z only for a given value of the applied voltage V . If the angle between the major axis of the molecules and the x -axis is denoted ϕ , the non-zero relative permittivity tensor elements of the LC are then $\varepsilon_{xx}^{(\text{LC})} = \varepsilon_1^{(\text{LC})}\cos^2\phi(V) + \varepsilon_3^{(\text{LC})}\sin^2\phi(V)$, $\varepsilon_{yy}^{(\text{LC})} = \varepsilon_2^{(\text{LC})}$, $\varepsilon_{zz}^{(\text{LC})} = \varepsilon_1^{(\text{LC})}\sin^2\phi(V) + \varepsilon_3^{(\text{LC})}\cos^2\phi(V)$, and $\varepsilon_{xz}^{(\text{LC})} = \varepsilon_{zx}^{(\text{LC})} = (\varepsilon_3^{(\text{LC})} - \varepsilon_1^{(\text{LC})})\cos\phi(V)\sin\phi(V)$. In the absence of applied voltage, the molecules of the LC tend to spontaneously organize themselves parallel to the (xz) plane, with a tilt angle ϕ assuming a value (called *pre-tilt angle*) close to 0° . Provided the voltage V applied between the electrodes increases to exceed a specific threshold value V_{th} (with $V_{\text{th}} \approx 1\ \text{V}$ in 5CB), the LC molecules rotate *non-uniformly* (with respect to abscissa z) within the cell because of their strong anchoring at each interface of the cell. In a large fraction of the cell, away from its boundaries, the tilt angle $\phi(z)$ remains close to its value in the center of the cell [27], all the more so when V assumes large values. For V just above the threshold voltage V_{th} , however, the spatial distribution of $\phi(z)$ is significantly non-uniform within the cell [23].

For $T < T_{\text{NI}}$, the dependence of the principal relative permittivities of 5CB upon temperature variations is nonlinear and can be approximated as $\varepsilon_i^{(\text{LC})} = A_i + B_i(\Delta\tilde{T}_i - T)^{1/2} + C_i(\Delta\tilde{T}_i - T) + D_i(\Delta\tilde{T}_i - T)^{3/2}$, $i = (1, 3)$, where $\Delta\tilde{T}_i = T_{\text{NI}} - \tilde{T}_i$. The numerical values used in section 3 for the empirical coefficients A_i , B_i , C_i , D_i , and \tilde{T}_i in 5CB can be found in [26]. The relative magnetic permeabilities of both ITO and LC are taken to be 1.

In the homogeneous magnetic film of cubic crystalline symmetry, the anisotropy is due to the magnetization. The magnetization vector being perpendicular to the surfaces of the film, there is no in-plane anisotropy and the x - and y -directions are equivalent. We take account of the bigyrotropic nature of YIG in the near-infrared regime (i.e. the dependence of its relative permittivity and permeability tensor elements $\varepsilon_{ij}^{(\text{YIG})}$ and $\mu_{ij}^{(\text{YIG})}$ on the local magnetization), as well as the linear magneto-electric coupling in the film. The latter is accounted for in the constitutive equations as follows: $D_i^{(\text{YIG})} = \varepsilon_0\varepsilon_{ij}^{(\text{YIG})}E_j^{(\text{YIG})} + \alpha\delta_{ij}H_j^{(\text{YIG})}$ and $B_i^{(\text{YIG})} = \mu_0\mu_{ij}^{(\text{YIG})}H_j^{(\text{YIG})} + \alpha\delta_{ij}E_j^{(\text{YIG})}$, where α is the linear magneto-electric constant of YIG and δ_{ij} is the Kronecker delta. The magneto-electric interaction needs to be taken into account, as it has been shown to noticeably modify the optical responses of magneto-optical effects in similar systems, in particular in thin YIG layers [7, 8, 11, 32]. In a first-order approximation, only the off-diagonal elements of the permittivity and permeability tensors depend on the local magnetization. In the polar magneto-optical configuration and at saturation magnetization, the tensor elements at room temperature are [1]: $\varepsilon_{jj}^{(\text{YIG})} = \varepsilon_0^{(\text{YIG})}$, $\mu_{jj}^{(\text{YIG})} = \mu_0^{(\text{YIG})}$ ($j = x, y, z$), $\varepsilon_{xy}^{(\text{YIG})} = -\varepsilon_{yx}^{(\text{YIG})} = i\varepsilon' m_z$ and $\mu_{xy}^{(\text{YIG})} = -\mu_{yx}^{(\text{YIG})} = i\mu' m_z$, where $\varepsilon_0^{(\text{YIG})}$ and $\mu_0^{(\text{YIG})}$ are the crystallographic elements of these tensors at room temperature, and $m_z = M/M_{\text{sat}} = \pm 1$. The temperature dependence of the diagonal permittivity tensor element of the magnetic film can be estimated as [23]: $\varepsilon^{(\text{YIG})}(\Delta T) \approx [n^{(\text{YIG})}(\Delta T)]^2 = (\sqrt{\varepsilon_0^{(\text{YIG})}} + \gamma^{(\text{YIG})}\Delta T)^2$. The

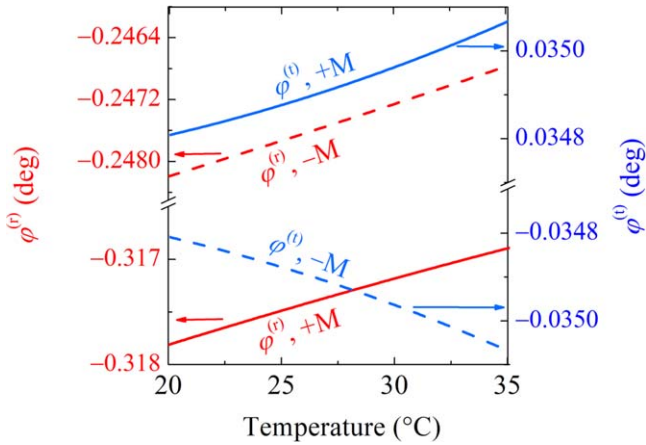


Figure 2. System: the magnetic film alone. Evolution of the Kerr angles $\varphi^{(r)}$ (red lines) and Faraday angles $\varphi^{(t)}$ (blue lines) with temperature for the magnetization vector in YIG film parallel (solid lines) and anti-parallel (dashed lines) to the z -axis.

thermal variations of the off-diagonal permittivity elements, as well as those of the permeability tensor elements, can be neglected.

The numerical values used in section 3 for YIG are $\varepsilon_0^{(\text{YIG})} = 5.0491$ [33], $\mu_0^{(\text{YIG})} = 1$, $\varepsilon' = -2.47 \times 10^{-4}$ and $\mu' = 8.76 \times 10^{-5}$ [34], $\alpha = 30 \text{ ps m}^{-1}$ [35], and $\gamma^{(\text{YIG})} = 2.5 \times 10^{-4} \text{ K}^{-1}$ [36].

Within the temperature range considered in this study, the relative increases of $\varepsilon^{(\text{ITO})}$ and $\varepsilon^{(\text{YIG})}$ are approximately 0.5% and 0.3%, respectively. This can be shown to be large enough to affect the optical response of the structure. However, the thermal dependence of the permittivity in the LC cell is much larger, with a 33% relative increase of $\varepsilon_1^{(\text{LC})}$ (from 6.3 to 8.4) and a 20% relative decrease of $\varepsilon_3^{(\text{LC})}$ (from 20.3 to 16.2) [23], which goes to show that the thermo-optic effect in the LC cell is predominant.

2.3. Derivation of the polarization plane rotation angles

In such an anisotropic system, the Kerr and Faraday effects do not simply result in a rotation of a plane of polarization of the s and p components of the incident field. For each of these components, magneto-optical and magneto-electric interactions in the system lead in the most general case to an elliptically polarized reflected or transmitted light. This is obviously also the case for any incident combination of s and p components, i.e. for any state of polarization of the incident beam.

The derivation of the polarization plane rotation angles is achieved with the well-established transfer matrix formalism [37] based on the resolution of Maxwell's equations, taking into account the constitutive equations of all materials. The overall transfer matrix of the system is obtained through the multiplication of interface matrices (derived from the boundary conditions at each interface of the system) and propagation (or dephasing) matrices in homogeneous layers. In the case of the inhomogeneous LC cell, the propagation matrix is derived by dividing the layer in thin sub-layers where the orientation of the molecules is in first

approximation assumed to be uniform. It is then immediate to derive the complex (2×2) reflection and transmission matrices $\hat{G}^{(r)}$ and $\hat{G}^{(t)}$ of the heterostructure, whose four, generally non-zero elements connect the amplitudes of the reflected (at $z = 0^-$) and transmitted (at $z = L^+$) field components to those of the incident wave (at $z = 0^-$) (figure 1):

$$\begin{aligned} E_p^{(r,t)} &= G_{pp}^{(r,t)} E_p^{(i)} + G_{ps}^{(r,t)} E_s^{(i)}, \\ E_s^{(r,t)} &= G_{sp}^{(r,t)} E_p^{(i)} + G_{ss}^{(r,t)} E_s^{(i)}, \end{aligned} \quad (1)$$

where subscripts p and s refer to the p - and s -polarizations, and superscripts (i) , (r) and (t) denote the incident, reflected and transmitted fields. The off-diagonal elements of the matrices $\hat{G}^{(r)}$ and $\hat{G}^{(t)}$ correspond to the cross-polarized contribution to the reflection and transmission due to the magneto-optical and magneto-electric properties of the magnetic layer described by ε' , μ' and α , respectively.

It remains convenient, however, to characterize and quantify the polarization changes of the reflected and transmitted light beams by using a set of two rotation angles, respectively, that can be calculated in terms of the reflection and transmission matrix elements, respectively, and defined as [38]:

$$\tan \varphi_s^{(r)} = -\text{Re} \left[\frac{G_{ps}^{(r)}}{G_{ss}^{(r)}} \right], \quad \tan \varphi_p^{(r)} = \text{Re} \left[\frac{G_{sp}^{(r)}}{G_{pp}^{(r)}} \right], \quad (2a)$$

$$\tan \varphi_s^{(t)} = -\text{Re} \left[\frac{G_{ps}^{(t)}}{G_{ss}^{(t)}} \right], \quad \tan \varphi_p^{(t)} = \text{Re} \left[\frac{G_{sp}^{(t)}}{G_{pp}^{(t)}} \right]. \quad (2b)$$

It should be noted that in the absence of the LC cell, $\varphi_{s,p}^{(r)}$ and $\varphi_{s,p}^{(t)}$ are pure Kerr and Faraday rotation angles. The presence of the LC cell does not produce any Kerr or Faraday effect since it is non-magnetic, nor does it induce any polarization plane rotation to s - and p -polarized incoming beams, as these are its polarization eigenstates. It does, however, influence the overall polarization plane rotation of the light reflected from and transmitted through the heterostructure via the interference of the beams bouncing back and forth between the interfaces of the system. Nevertheless, we will hereon refer to $\varphi_{s,p}^{(r)}$ and $\varphi_{s,p}^{(t)}$ as the Kerr and Faraday angles, as they originate in the magneto-optical effects taking place in the YIG magnetic layer.

The elements of the reflection and transmission matrices, and thus the values of $\varphi_{s,p}^{(r)}$ and $\varphi_{s,p}^{(t)}$, are determined by the elements of permittivity and permeability tensors of the system constituents, as well as by the layer thicknesses. Thus changes in polarization will depend on the voltage applied to the LC cell, as well as on temperature through thermal expansion and the thermo-optic effect.

3. Simulation results and discussion

3.1. Magnetic film alone

First we study the polarization plane rotation at normal incidence for the sole magnetic film, i.e. when no LC cell is

present in the system. Figure 2 shows the temperature dependence of the Kerr and Faraday angles for two orientations of the magnetization vector in the film: parallel ($m_z = +1$) and anti-parallel ($m_z = -1$) to the z -axis.

Note that at normal incidence, due to the absence of in-plane anisotropy in the polar magneto-optical configuration, there is no difference between the s - and p -polarizations. In that case, $G_{sp}^{(r,t)} = G_{ps}^{(r,t)}$ and $G_{pp}^{(r,t)} = -G_{ss}^{(r,t)}$, so that $\varphi_p^{(r)} = \varphi_s^{(r)} \equiv \varphi^{(r)}$ and $\varphi_p^{(t)} = \varphi_s^{(t)} \equiv \varphi^{(t)}$.

As is expected in the polar magneto-optical configuration, the Faraday angles $\varphi^{(t)}$ change sign under the magnetization reversal and increase when the temperature increases from T_0 to T_{NI} . The Kerr angles $\varphi^{(r)}$ have the same negative sign for both directions of \mathbf{M} and decrease in absolute value in the same temperature range. However, for this sole magnetic film, the rate of temperature-induced polarization changes is only about $10^{-4} \text{ }^\circ\text{C}^{-1}$ for $\varphi^{(r)}$ and $2 \times 10^{-5} \text{ }^\circ\text{C}^{-1}$ for $\varphi^{(t)}$. It should be noted that the sign change of the Faraday angle φ^F upon magnetization reversal from the parallel to the anti-parallel polar configuration is non-symmetrical, since $G_{ps,sp}^{(t)}(+\mathbf{M}) \neq -G_{ps,sp}^{(t)}(-\mathbf{M})$, which is due to the magneto-electric interaction in the film—whereas $G_{ps,sp}^{(t)}(+\mathbf{M}) = -G_{ps,sp}^{(t)}(-\mathbf{M})$ in the absence of that interaction, i.e. for $\alpha = 0$. Magnetization reversal results in an almost constant jump—about 0.07° —of the value of the Kerr angle $\varphi^{(r)}$ over the whole temperature range. The corresponding jump of the value of the Faraday angle $\varphi^{(t)}$, although it slightly increases in absolute value with temperature, also does not exceed 0.07° .

In any case, for this system consisting of a sole magnetic film, the only way to affect the value of the magneto-optical effects at a given ambient temperature is to reverse the saturation magnetization. This is not sufficient if an effective tunability of these effects is to be achieved. In that perspective, at least one additional functional constituent needs to be included in the system.

3.2. Combined LC cell and magnetic film

As previously stated, in what follows we will consider such an additional constituent to be a voltage-controlled LC cell deposited on top of the magnetic film. Its presence is meant to result in both an overall increase of the Kerr and Faraday angles and an increase of their dependence on temperature. Additionally, the variation of the optical properties of the LC with the dc voltage established between the electrodes provides a further means of control of the magneto-optical responses of the heterostructure.

The addition of the anisotropic, heterogeneous LC cell, however, makes these responses more complex than those of the YIG film alone. In particular, due to the in-plane anisotropy of the LC, neither the Kerr angle nor the Faraday angle are any longer the same for s - and p -polarized light at normal incidence. Note that this is true even for values of the applied dc voltage V below the characteristic threshold voltage V_{th} . As mentioned above, the molecules of the LC tend to organize themselves parallel to the (xz) plane, and as soon as $V > V_{th}$,

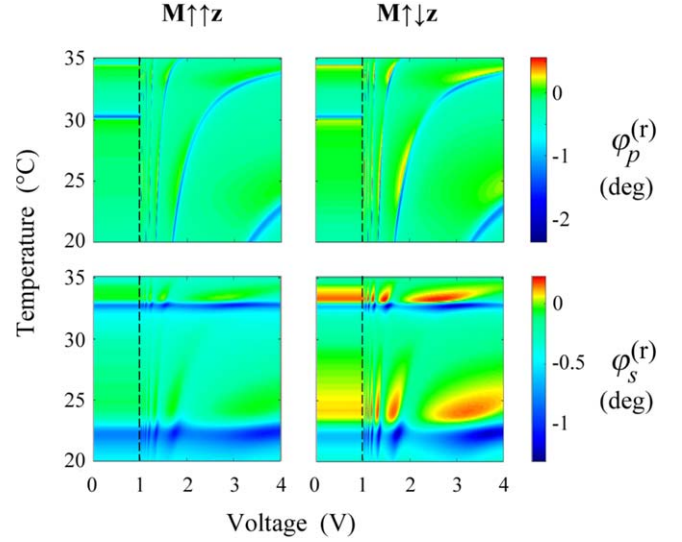


Figure 3. System: LC cell on magnetic film. Evolution of Kerr angles $\varphi_p^{(r)}$ (top) and $\varphi_s^{(r)}$ (bottom) with temperature and applied voltage for a magnetization vector in the YIG film parallel (left column) and anti-parallel (right column) to the z -axis. The vertical black dashed lines denote the threshold voltage V_{th} .

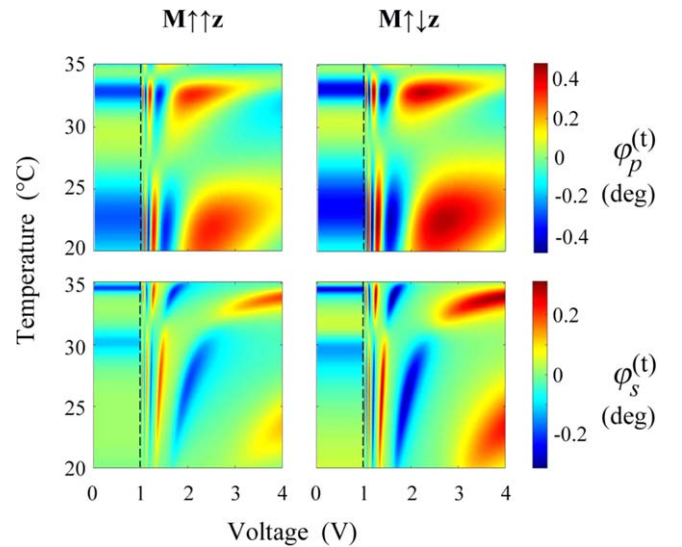


Figure 4. System: LC cell on magnetic film. Evolution of Faraday angles $\varphi_p^{(t)}$ (top) and $\varphi_s^{(t)}$ (bottom) with temperature and applied voltage for a magnetization vector in the YIG film parallel (left column) and anti-parallel (right column) to the z -axis. The vertical black dashed lines denote the threshold voltage V_{th} .

they rotate, still parallel to that plane, with a tilt angle ϕ with respect to the x -axis increasing from the so-called pre-tilt angle (close to 0°) towards the asymptotic value of 90° . Consequently, the LC cell exhibits an in-plane anisotropy for all values of V .

Figures 3 and 4 show the dependence of the Kerr and Faraday angles, respectively, for both an s -polarized and a p -polarized incident light beam, and for a magnetization vector in the YIG film either parallel (left column) or anti-parallel (right column) to the z -axis.

Figure 3 clearly shows the very different behaviour of $\varphi_s^{(r)}$ and $\varphi_p^{(r)}$ with respect to the temperature and the applied voltage. If, as expected, neither of these angles depends on the voltage below V_{th} , it can also be seen that even at $V = 0$, the variations of the Kerr angles do not reproduce the monotonous dependence with temperature that was obtained with the sole magnetic film (see figure 2), which can be related to the different temperature dependences of the permittivity tensor elements of the anisotropic LC (see section 2.2).

In the parallel polar configuration, the Kerr angles keep negative values, as they did for the sole magnetic film. They reach, however, substantially larger levels, up to 2° in absolute value. Let us notice that for $\varphi_s^{(r)}$, these larger values are limited to some temperature ranges (around 22.5°C and 33°C) and do not change much with the applied voltage. For $\varphi_p^{(r)}$, in contrast, similar larger negative values can be reached at all temperatures, but only within specific and narrow domains of the applied voltage.

Upon magnetization reversal in the YIG film from the parallel to the anti-parallel polar configuration, the variations of both Kerr angles do not change qualitatively (their negative extrema, around -1.5° , are reached within the same domains of temperature and applied voltage as in the parallel configuration), but overall their absolute values are reduced. They can even assume positive values in temperature and voltage domains where they were near-zero in the parallel polar configuration. The positive maxima, however, do not exceed 0.5° .

Some of the same observations can be made for the Faraday angles (figure 4), in particular the fact that their variation with temperature with no voltage applied to the LC cell (indeed, for all voltage values below threshold V_{th}) is, again, nonmonotonous, unlike what can be observed for the sole YIG film. Similarly, the variations of $\varphi_s^{(t)}$ and $\varphi_p^{(t)}$ with temperature and applied voltage are markedly different. However, differences with the behaviour of the Kerr angles can also be noted. Indeed, as was the case for the sole magnetic YIG film, the Faraday angles do not change sign upon magnetization reversal. The latter only leads to a slight increase of the absolute values of the rotation angles, which can, depending on the temperature and voltage, be positive as well as negative. Overall, however, the extrema of $\varphi_s^{(t)}$ and $\varphi_p^{(t)}$ in the presence of the LC cell do not exceed 0.4° in absolute value—an increase rate, as compared to the case of the sole magnetic film, 5 times smaller than for the Kerr angles.

For both Kerr and Faraday rotations, as was hoped for, the inclusion of the LC cell to the system brings a versatility that allows one to tune the values of the rotation angles for s - as well as for p -polarized incident light. These values can be annulled or, indeed, increased, by playing on the dc voltage applied to the LC cell as well as on the direction of the saturation magnetization in the YIG film. It must be noted, however, that larger rotation angles can be achieved for the Kerr rotation than for the Faraday rotation.

It can be of particular interest to study in more detail the variations of the Kerr and Faraday angles in the near-threshold domain of dc voltage V , if only because it would be

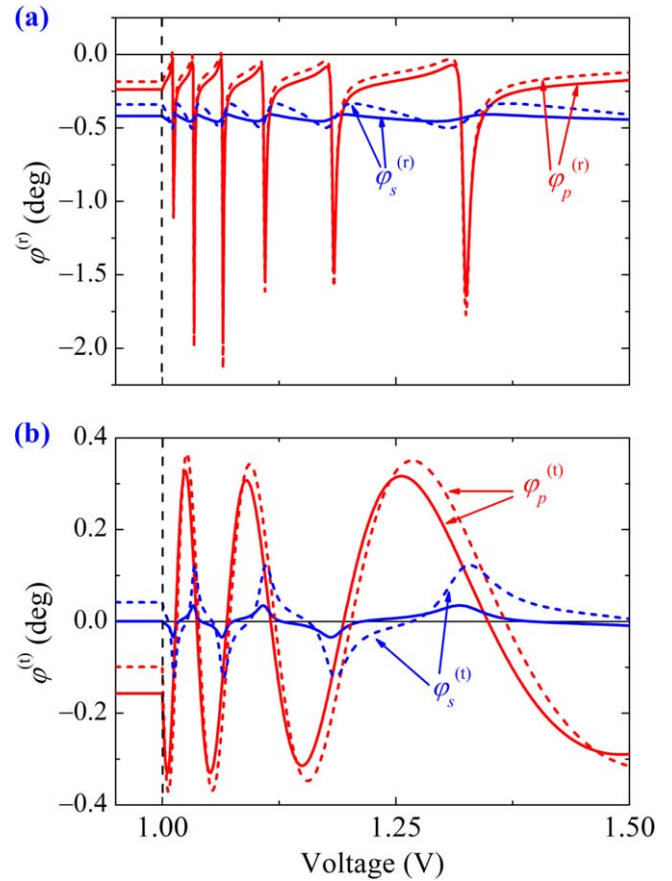


Figure 5. System: LC cell on magnetic film. Cross-sections of figures 3 and 4 at $T = 20^\circ\text{C}$ in the vicinity of V_{th} : (a) Kerr angles and (b) Faraday angles for p -polarized (red lines) and s -polarized (blue lines) incident light. The coloured solid and dashed lines correspond to the parallel and anti-parallel polar configurations for the magnetization vector in the YIG film, respectively. The vertical black dashed lines denote the threshold voltage V_{th} .

desirable that any potential application of the measurement of those angles should require as low an externally applied voltage as possible. The domain just above the voltage threshold (say, up to 1.5 V) is also interesting because the variations of the magneto-optical rotation angles can be particularly drastic in that region. In other words, and keeping in mind potential applications to temperature sensing, the sensitivity of these angles to temperature shifts and to a control through the applied voltage is high in the near-threshold region.

Let us first notice that unlike what may appear at first glance in some of the panels of figures 3 and 4, there is obviously no discontinuity in the calculated Kerr and Faraday angles when V crosses its threshold value V_{th} . This is clearly visible in figure 5, where the variations of these four angles have been plotted between $V = 0.95\text{ V}$ (i.e. just below V_{th}) and $V = 1.5\text{ V}$, at $T = 20^\circ\text{C}$ and in the parallel and anti-parallel polar configuration of magnetization in the YIG film.

Figure 5 illustrates the typical complex and fast changes that Kerr and Faraday rotation angles experience in this system when the voltage applied to the LC cell increases just above V_{th} and the following comments remain for the most

part valid when temperatures increases from T_0 to T_{NI} . For both Kerr and Faraday rotations, larger absolute values are obtained for maxima of the rotation angles when the incident beam is p -polarized than when it is s -polarized, which makes the former configuration more interesting. In both cases as well, a reversal of magnetization in the YIG film from the parallel to the anti-parallel configuration slightly increases the absolute value of the rotation angle maxima. Their positions (in terms of applied voltage) only slightly change towards larger values of V , more so for the Faraday than for the Kerr rotation. As could already be seen in figures 3 and 4, the maximal absolute values reached by the Kerr angle are significantly larger (some five times larger at 20 °C and for a p -polarized incident beam) than those reached by the Faraday angle. However, it should be noted that for p -polarized incident light the maxima, in absolute value, of the Kerr angle correspond to near-zero minima of the reflection coefficients $G_{pp}^{(r)}$ and $G_{ss}^{(r)}$ (thus to minima of the reflected beam intensity) whereas those of the Faraday angle coincide with maxima of the corresponding transmission coefficients $G_{pp}^{(t)}$ and $G_{ss}^{(t)}$, and of the transmitted beam intensity. Consequently, for all intents and purposes, the Faraday rotation is better suited than the Kerr rotation to a voltage control of the magneto-optical response of the structure. This conclusion is reinforced by the fact that the absolute maxima of the Kerr angles manifest themselves as a set of much narrower peaks (figure 5(a)) than those leading to absolute maxima of the Faraday angles (figure 5(b)), which means that reaching the former necessitates a much more precise control of the applied voltage.

Furthermore, for any practical application of the Faraday rotation, the relevant parameter is the rotation angle per unit of thickness of the magnetic medium. The simulation results shown in figure 2, where the system under study is the sole thin YIG layer, put this parameter at about 120°cm^{-1} , which is of the same order of magnitude as measurements carried out with thicker YIG slabs at similar temperatures [39, 40]. As has been observed in figures 4 and 5, the addition of the voltage-controlled LC cell to the YIG film can lead to a significant enhancement of the Faraday rotation by a factor of approximately 15 for the range of temperatures and applied voltages considered in this study.

However, as could be seen in figures 3 and 4, if adjoining the LC cell to the magnetic YIG film does indeed allow significantly larger and tunable values of the magneto-optical Kerr and Faraday angles, it also introduces a strong and complex sensitivity of those responses to even small temperature changes—much stronger and, above all, much more complex than in the magnetic film alone (see figure 2). As a consequence, using this structure as a way to enhance and control the magneto-optical responses of the magnetic film requires drifts in temperature to be taken into account, if not controlled, let alone avoided.

On the other hand, contrary to the YIG film alone, this structure provides a way to compensate for those drifts, and for the dramatic changes in magneto-optical responses they induce, by tuning the voltage applied to the LC cell. This can be seen in figure 6, where iso-valued contours obtained from

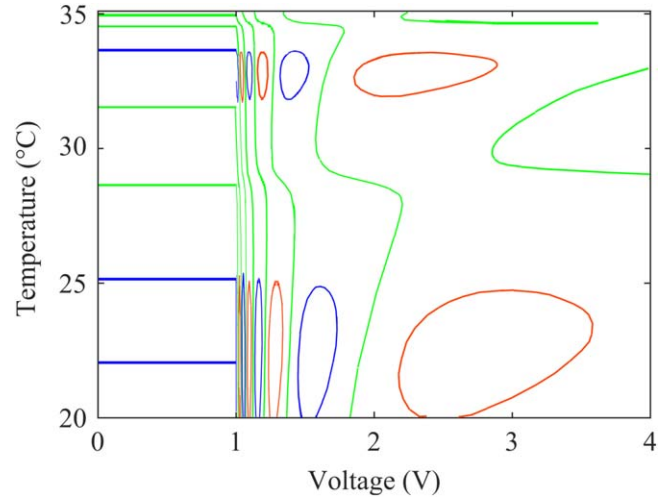


Figure 6. System: LC cell on magnetic film. Isovalued contours of the Faraday angle obtained for p -polarized incident light and in the anti-parallel polar configuration of magnetization in the YIG film: for $\varphi_p^{(i)} = -0.3^\circ$ (blue lines), $\varphi_p^{(i)} = 0$ (green lines), and $\varphi_p^{(i)} + 0.3^\circ$ (red lines).

the top right hand side panel of figure 4 display the dependence of the Faraday angle $\varphi_p^{(t)}$ in the anti-parallel polar magnetization configuration of the YIG film (i.e. for a choice of magneto-optical response, incident state of polarization and magnetic configuration best suited to potential practical applications, as we concluded in our discussion of figure 5) for three values of that angle ($\varphi_p^{(i)} = -0.3^\circ, 0^\circ$ and $+0.3^\circ$). Similar plots are readily obtained for any other value of $\varphi_p^{(i)}$, as well as if the magneto-optical response of interest is $\varphi_s^{(t)}$ or Kerr angles $\varphi_s^{(r)}$ and $\varphi_p^{(r)}$.

These contours show that for any application aiming to exploit the ability to use the control of the magneto-optical response of the heterostructure provided by the dc voltage V applied to the LC cell, drifts of the setpoint (here, the Faraday or Kerr angle the user wishes to obtain) resulting from temperature drifts can indeed be corrected with a slight adjustment of V .

4. Conclusions

In this paper, we have developed a theoretical study of the influence of temperature on the polarization rotations of a near-infrared beam impinging, under normal incidence, on a voltage-controlled nematic LC cell deposited on a magnetic YIG film magnetized at saturation in the polar magneto-optic configuration. The influence of temperature has been considered in terms of both the thermal expansion of the layers constituting the system and the thermo-optic effect responsible for thermally driven changes in the permittivity tensor components of its constituents, with temperatures ranging from room temperature (20 °C) to the nematic-isotropic phase transition temperature (35.1 °C) of the LC.

The results of our modelization show that the combination of temperature changes and limited variations of the

voltage applied to the LC cell can lead to a noticeable enhancement of polarization plane rotation angles of both reflected and transmitted light. On the other hand, this combined sensitivity can be used in order to maintain the magneto-optical response of the magnetic film when temperature varies by tuning the applied voltage. Furthermore, our results suggest the feasibility of using the magneto-optical response (in particular the Faraday rotation) as a way to design a sensitive temperature monitoring device.

Acknowledgments

This work is supported in part by the Ministry of Science and Higher Education of the Russian Federation (Project No. 3.7614.2017/9.10), Regional Council of Brittany, France (Project SPEACS), and by École Nationale d'Ingénieurs de Brest (Project HF-CCCP).

ORCID iDs

Yuliya S Dadoenkova  <https://orcid.org/0000-0001-9648-6583>

Florian F L Bentivegna  <https://orcid.org/0000-0003-1793-2157>

Sergey G Moiseev  <https://orcid.org/0000-0001-8252-7997>

References

- [1] Zvezdin A K and Kotov V A 1997 *Modern Magneto-optics and Magneto-optical Materials* (Bristol: Institute of Physics Publishing)
- [2] Mansuripur M 1995 *The Physical Principles of Magneto-Optical Recording* (Cambridge: Cambridge University Press)
- [3] Gräfe J, Schmidt M, Audehm P, Schütz G and Goering E 2014 *Rev. Sci. Instrum.* **85** 023901
- [4] Atatüre M, Dreiser J, Badolato A and Imamoglu A 2007 *Nat. Phys.* **3** 101
- [5] Dissanayake N, Levy M, Chakravarty A, Heiden P A, Chen N and Fratello V J 2011 *J. Appl. Phys.* **99** 091112
- [6] Chen K-L, Lin Y-S, Chen J-M, Wu C-H, Jeng C-C and Wang L-M 2018 *Sensors Actuators B* **258** 947
- [7] Dadoenkova Y S, Lyubchanskii I L, Lee Y P and Rasing T 2010 *Appl. Phys. Lett.* **96** 011901
- [8] Dadoenkova Y S, Lyubchanskii I L, Lee Y P and Rasing T 2011 *IEEE Trans. Magn.* **47** 1623
- [9] Dadoenkova Y S, Lyubchanskii I L, Lee Y P and Rasing T 2012 *J. Magn. Soc. Japan* **36** 32
- [10] Goto T, Baryshev A V, Tobinaga K and Inoue M 2010 *J. Appl. Phys.* **107** 09A946
- [11] Dadoenkova Y S, Dadoenkova N N, Lyubchanskii I L, Kłos J and Krawczyk M 2017 *IEEE Trans. Magn.* **53** 2501005
- [12] Loughran T H J, Keatley P S, Hendry E, Barnes W L and Hicken R J 2018 *Opt. Express* **26** 4738
- [13] Ono K et al 1995 *J. Magn. Magn. Matter.* **148** 74
- [14] Bang D, Awano H, Saito Y and Tominaga J 2016 *AIP Adv.* **6** 055810
- [15] Bang D, Awano H, Saito Y and Tominaga J 2016 *J. Electron. Mater.* **45** 2496
- [16] Li Y, Han W, Swartz A G, Pi K, Wong J J I, Mack S, Awschalom D D and Kawakami R K 2010 *Phys. Rev. Lett.* **105** 167203
- [17] Wittekoek S and Rinzeema G 1971 *Phys. Status Solidi b* **44** 849
- [18] Sato H, Kawase M and Saito M 1985 *Appl. Opt.* **24** 2300
- [19] Mihailovic P M, Petricevic S J and Radunovic J B 2013 *IEEE Sensors J.* **13** 832
- [20] Li X, Liu P, Li G, Guang X, Xu Z, Guan L and Li G 2017 *Sensors* **17** 2046
- [21] Ahn J Y, Tanaka M and Imamura M 2001 *J. Appl. Phys.* **89** 7395
- [22] Snetkov I L 2018 *IEEE J. Quantum Electron.* **54** 7000108
- [23] Dadoenkova Y S, Bentivegna F F L, Petrov R V and Bichurin M I 2018 *J. Appl. Phys.* **123** 033105
- [24] Dadoenkova Y S, Bentivegna F F L, Svetukhin V V, Zhukov A V, Petrov R V and Bichurin M I 2017 *Appl. Phys. B* **123** 107
- [25] Dadoenkova Y S, Bentivegna F F L, Petrov R V and Bichurin M I 2017 *J. Opt.* **19** 095802
- [26] Bogi A and Faetti S 2001 *Liq. Cryst.* **28** 729
- [27] Abdulhalim I and Menashe D 2010 *Liq. Cryst.* **37** 233
- [28] König T A F, Ledin P A, Kerszulis J, Mahmoud M A, El-Sayed M A, Reynolds J R and Tsukruk V V 2014 *ACS Nano* **8** 6182
- [29] Bhattacharyya D and Carter M J 1996 *Thin Solid Films* **288** 176
- [30] Ahlers G 1995 *Experiments on Thermally Driven Convection* (Berlin: Springer)
- [31] Socorro A B, Soltani S, Del Villar I, Corres J M and Armani A M 2015 *Opt. Express* **23** 1930
- [32] Fiebig M 2005 *J. Phys. D: Appl. Phys.* **38** R123
- [33] Hellwege K-H and Hellwege A M (ed) 1978 *Landolt-Börnstein—Group III, Condensed Matter, Magnetic and Other Properties of Oxides and Related Compounds—Part A: Garnets and Perovskites* vol 12a (Berlin: Springer)
- [34] Torfeh M and Le Gall H 1981 *Phys. Status Solidi a* **63** 247
- [35] Krichevstov B B, Pavlov V V, Pisarev R V and Selitsky A G 1993 *Ferroelectrics* **161** 65
- [36] Shoji Y, Nemoto T and Mizumoto T 2014 *Proc. IEEE Photonics Conf.* p 589
- [37] Born M and Wolf E 1999 *Principles of Optics* (Cambridge: Cambridge University Press)
- [38] Du Trémolet de Lacheisserie É, Gignoux D and Schlenker M (ed) 2005 *Magnetism* (Boston: Springer)
- [39] Imaeda M and Kozuka Y 1992 *Proc. 8th Optical Fiber Sensors Conf.* p 386
- [40] Cooper R W, Crossley W A, Page J L and Pearson R F 1968 *J. Appl. Phys.* **39** 565